Fachtagung "Experimentelle Strömungsmechanik"
5.–7. September 2023, München

Charakterisierung des Geschwindigkeits- und Temperaturfeldes in einem akustisch angeregten Mikrokanal mit inhomogener Temperaturverteilung

On the characterization of the velocity and temperature fields in an acoustically driven microchannel with non-uniform temperature distribution

F. Martens[1], W. Qiu[1], P. Augustsson[1], C. Cierpka[2,*]

1) Department of Biomedical Engineering, Lund University, Lund, Sweden
2) Institute of Thermodynamics and Fluid Mechanics, Technische Universität Ilmenau
* Visiting research fellow at Department of Biomedical Engineering, Lund University

Keywords: acoustofluidics, particle tracking, luminescence lifetime imagining

Summary

In this study a system to measure the volumetric temperature distribution in a microchannel was applied using life time imaging of temperature sensitive particles. The system of interest is a microchannel which is acoustically excited by a piezo-electric transducer. In addition, a temperature gradient is generated inside the fluid using a focused near-infrared laser and a dye, dilluted in water, to absorb the infrared light as fluid. The temperature gradients result in different acoustic properties in the system, drivinga complex streaming flow which acts in addition to the acoustic radiation force on particles in the channel. The channel is equipped with a PT100 sensor and a peltier element for precise temperature control to establish a calibration. For the measurements, the timing scheme and calibration procedure are adapted to the standard method to cope with the rolling shutter and photobleaching effects. Preliminary results show a mean temperature increase in the middle of the channel of ~ 0.3 K within 30 seconds. Furthermore, the measurements indicate the typical time scales and amplitudes of the temperature rise of the whole system and pave the ground for further, more detailed investigations.

Introduction

Particles and cells can be manipulated exploiting acoustic fields in microchannels using bulk acoustic waves or surface acoustic waves (Sachs et al. 2022, Weser et al. 2022). For the generation of a bulk acoustic wave in the channel a piezoelectric transducer driven with an AC voltage with frequencies in the lower MHz range is fixed to a microfluidic chip. Particles within this fluid are then affected by the sound pressure distribution directly via the acoustic radiation force (ARF) and by the drag force due to acoustic streaming (AS). As the ARF scales for constant material properties with the volume, it is often used for the separation of particles and cells. However, inhomogeneities in density and compressibility in the fluid can change the forces considerably (Karlsen et al. 2016). Such inhomogeneities can be produced by thermal gradients (Qiu et al. 2018). For the current setup this is accomplished by heating a small region in a microchannel with a cross-section of 375 × 150 μm^2 with an infrared laser (wavelength of 785 nm) from below (see Fig. 2). This approach furthermore offers the flexibility to manipulate the temperature distribution in time and space. To increase the energy that is absorbed, Indio-Cyanin green (ICG) dye is added to the fluid which additionally allows to control the amount of absorption by adjusting the dye concentration. The streaming flow is measured for different

GALA e.V., Karlsruhe, Germany, ISBN 978-3-9816764-9-5

dye concentrations at identical laser power. Small particles (d_P = 2 µm) are suspended in the flow and their movement was determined using astigmatism particle tracking. The illumination is achieved using a high-power LED with a wavelength peaked at 470 nm. Particle images are recorded by a back illuminated Orca Fusion sCMOS camera with a frame rate of 20 Hz. The data evaluation is either performed with a correlation approach or the direct evaluation of the particle image shapes and delivers the full three-dimensional velocity field (Barnkob et al. 2021).
Surprisingly, the velocity fields show remarkable differences for different dye concentrations. In the upper row of Fig. 1., 3D representations of the velocity fields are shown. The streamlines indicate the velocity magnitude for a dye concertation of 0.001mg/ml ICG in MilliQ filtered water, leading to an absorption of 50% (left) and 0.01mg/ml ICG in MilliQ filtered water leading to an absorption of 100 % (right). As can be seen the streaming field seem qualitatively very similar. However, the magnitude is lower (note different colour scales) for the higher concentration, which is counter-intuitive and was not observed for other concentrations. In addition, the out-of-plane velocity also shows qualitative differences as can be seen by the different color distributions in the lower row. This effect migth have been due to aging of the dye or other mechanisms. In any case a temperature measurments will help to reveal the complex physics of the system.

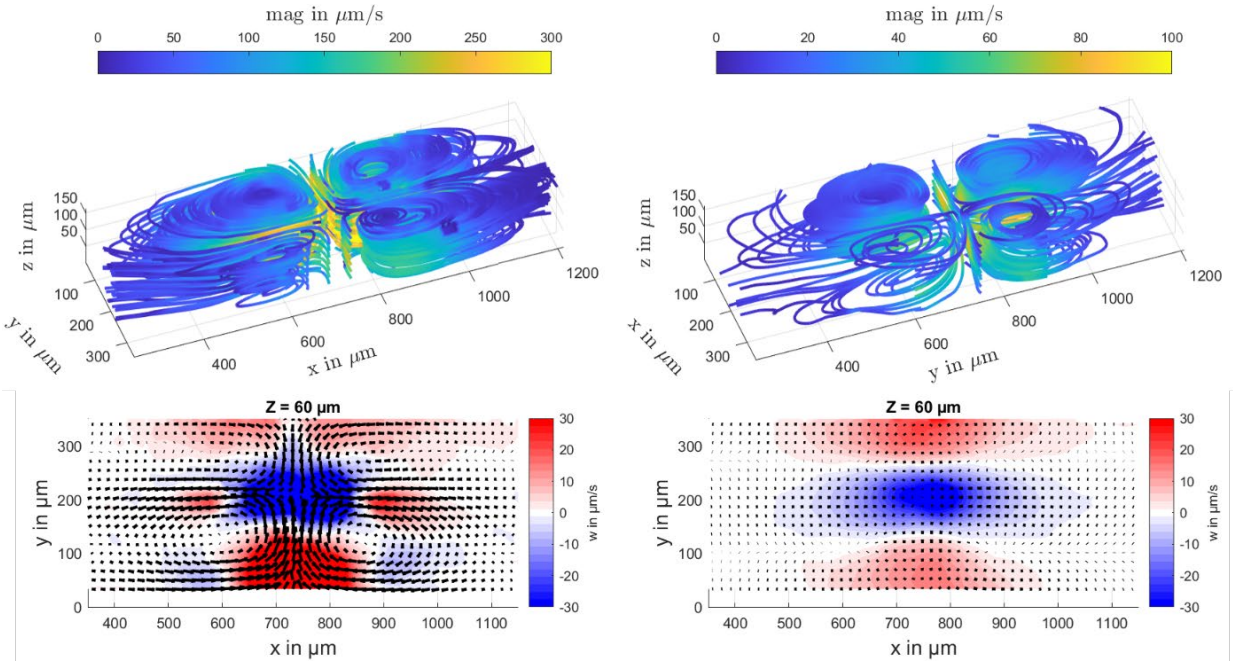

Fig. 1 Upper row: 3D representation of the flow by streamlines for a dye concentration leading to an absorption of 50% (left) and 100 % (right). Lower row: Top-view of the in-plane streaming velocity (vectors) and the corresponding out-of-plane velocity (colour) at z = 60 µm using a dye concertation leading to an absorption of 50% (left) and 100 % (right).

Temperature measurements

The key to further understand the streaming field would be the characterization of the temperature distribution inside the channel. The implementation of a luminescent lifetime imaging method using an UV illumination (Thorlabs SOLIS-365C) and temperature sensitive particles is currently under way [4]. In Fig. 2 the changes made to the setup are highlighted in red. The LED was exchanged with an LED that excites the temperature sensitive particles (Surflay Nanotec, d_p = 10 µm) in the UV range (peak wavelength 365 nm). In order to allow for a temperature calibration a Peltier element was installed close to the channel. The heat was distributed towards the channel by an alluminum heat conductor plate, contacting the channel close to the field of view from the side as the channel needed to remain transparent for illumination and imaging. For the control of the Peltier element a Pt100 temperature sensor was installed in the vicinity (see insert bottom rigth in Fig. 2). The temperature of the system

GALA e.V., Karlsruhe, Germany, ISBN 978-3-9816764-9-5

can be controled by a Meerstetter PID controler type TEC-1091. For the luminescent lifetime imaging the particles have to be excited in the first frame until saturation. While the LED is switched of during the second frame, the intensity in this frame is a measure for the lifetime of the luminescence (Massing et al. 2018, Deng et al. 2022). The timing of the camera with respect to the LED was ensured by a Digilent Analog Discovery 2 oscilloscope and trigger that allows for easy programming of different timing schemes (not shown).

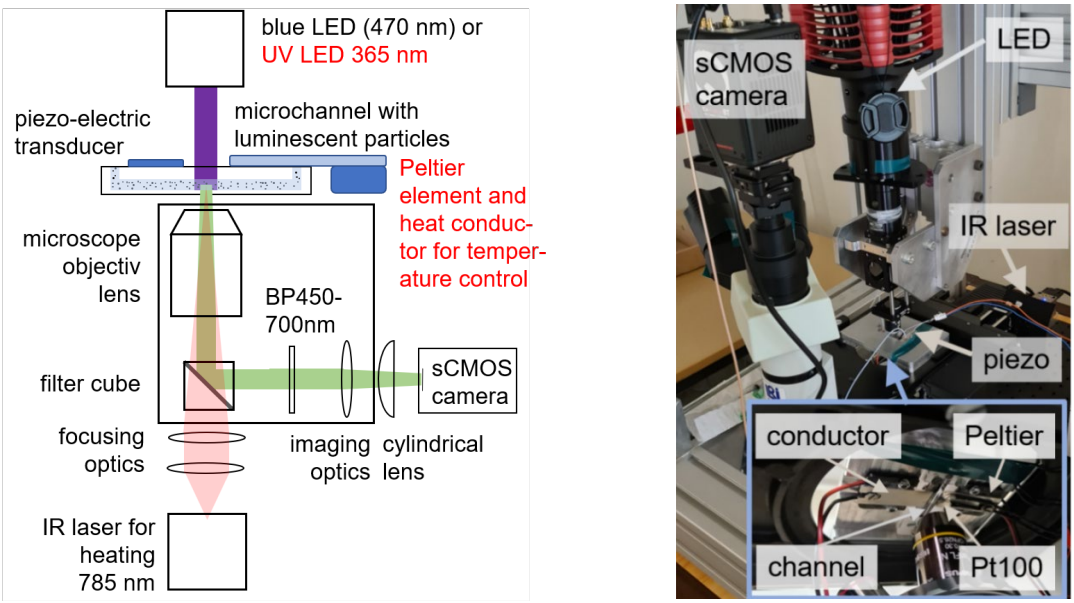

Fig. 2: Schematic of the setup for the temperature measurements (left) and photograph (right). The illumination is from the top through the channel whereas the NIR laser spot and the particle observation are established from the bottom through a microscope objective lens.

In order to get a rough idea on the different time scales of the system, the temperature reading of the Pt100 over time is presented for different conditions in Fig. 3. First, the system was at rest at a temperature slightly below 20.5 °C. When the NIR laser was switched on a slight increase in temperature by 0.04 K in about one minute can be observed. The application of the sound field by the piezo-electric transducer increases the temperature again for 0.1 K. Finally, the blue LED was switched on permanently which resulted in a more sudden increase in temperature of the system of about 0.15 K. When everything was switched off, the system fell back to room temperature within several minutes. An increase in laser power from t = 7.5 min resulted in a much higher temperature rise but with the same time scale of about 1 minute. Finally, the temperature control was switched on, which after some overshoot stabilized the temperature at. 20.5 °C reliably. From these preliminary measurements it can be concluded that the time scale for the process to be in steady conditions is in the order of ~ 1 min, which is important for the measurements.

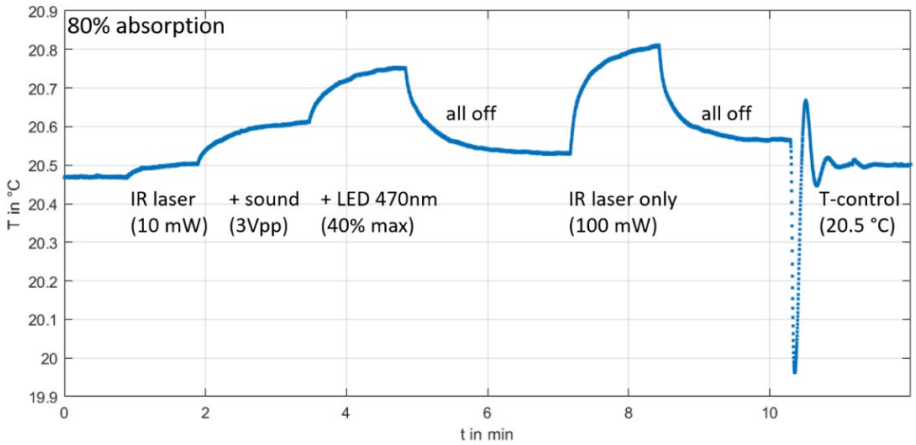

Fig. 3: Temperature measured by the Pt100 thermistor vs. time for different operating conditions.

GALA e.V., Karlsruhe, Germany, ISBN 978-3-9816764-9-5

In order to avoid further heating through the LED a timing scheme was chosen that the LED is only active for 20 ms within 100 ms of the total time. Furthermore, only a current of 300 mA (corresponding to an output power of 0.3 W or 7.5% max) was chosen. This timing scheme resulted in only 0.01 K temperature increase for the 50 seconds of measurement time evaluated to test the amount of photobleaching. In Fig. 4 the normalized intensity in frame 1 for ~ 10 particles in two consecutive experiments are shown in red. It is obvious that photobleaching significantly decreased the intensity in the first frame by up to 20% for 500 double frames (equivalent to 10 s illumination with the above given settings). Furthermore, the photobleaching seems to be different for different particles. However, the ratio of the intensities between frame 1 and frame 2 (black points in Fig. 4) show only a minor decrease. However, it can be seen that the variance increases as well due to the fact that with lower signal-to-noise ratio also the variance of the intensity ratio increases. The conclusions drawn for the timing scheme of the actual measurements are, that photobleaching has to be avoided and if long-time measurements are to be performed the frame rate has to be reduced to avoid large number of exposures (< 1000 double frames).

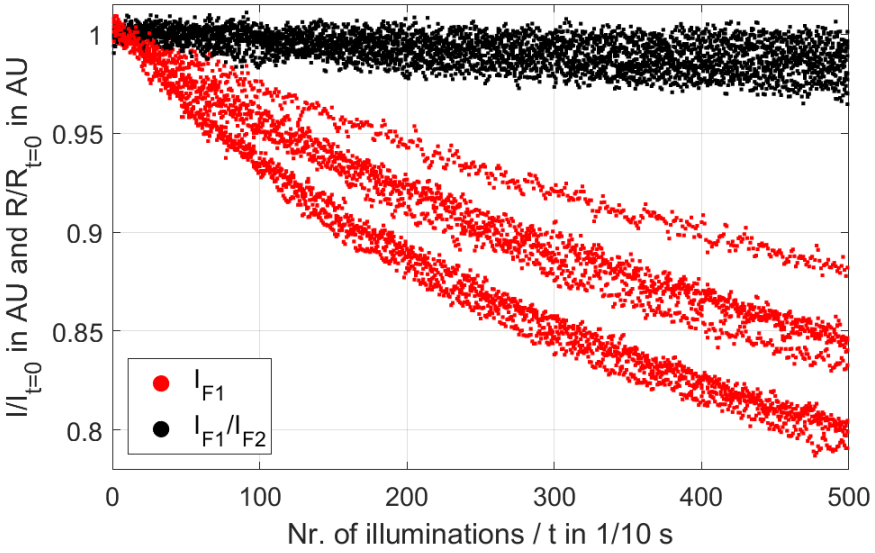

Fig. 4: Normalized intensity in the first frame (red) and intensity ratio (black) vs. the number of illuminations indicating photobleaching for an intensity measurement and a stable signal for the ratiometric approach.

The calibration procedure had to be adopted using the current camera as it does not feature a global shutter. This means that a slight difference in timing occurs for the exposure and read-out of successive pixel lines (~5 to 10 µs per line). In consequence, the ratio *R* of the intensity between first and second frame is not uniform throughout the whole field of view but is a function of the *y*-position. Furthermore, the time difference between the successive frames is in the order of several microseconds, which lowers the signal in the second frame and results in further uncertainties. The ratio and thus the determined temperature are therefore a function of the position in the image and furthermore to a certain extend dependent on the individual particle. For the calibration the temperature controller was set up to generate a sinusoidal temperature over time in the range between 20 and 40 °C as this was expected from a first numerical model. The sinusoidal signal allows to find the temporal correspondence as the system was not externally synchronized and furthermore allows to double check if photo bleaching occurs (Deng et al, 2022). Since the photobleaching was not severe, no correction was done.
In Fig. 5 the reconstruction of the temperature field by the calibration with a sinusoidal set temperature is shown. A second order polynomial fit for the gradient and offset, determined for each particle individually, was used. This approach considers individual differences for the calibration as well as differences due to the rolling shutter. There are no systematic errors as the temperature field is well reconstructed for the *x*- and *y*-direction (upper two graphs) and in time (lower graph), respectively. The mean deviation between measured and set temperature was 0.15 K. However, the standard deviation for individual particles is 4.7 K. The determined calibration was used for a different particle distribution with the same settings for the recording. The results in Fig. 6 show that in general the temperature can be derived, however, due to slight differences for individual particles, the deviation increases slightly.

GALA e.V., Karlsruhe, Germany, ISBN 978-3-9816764-9-5

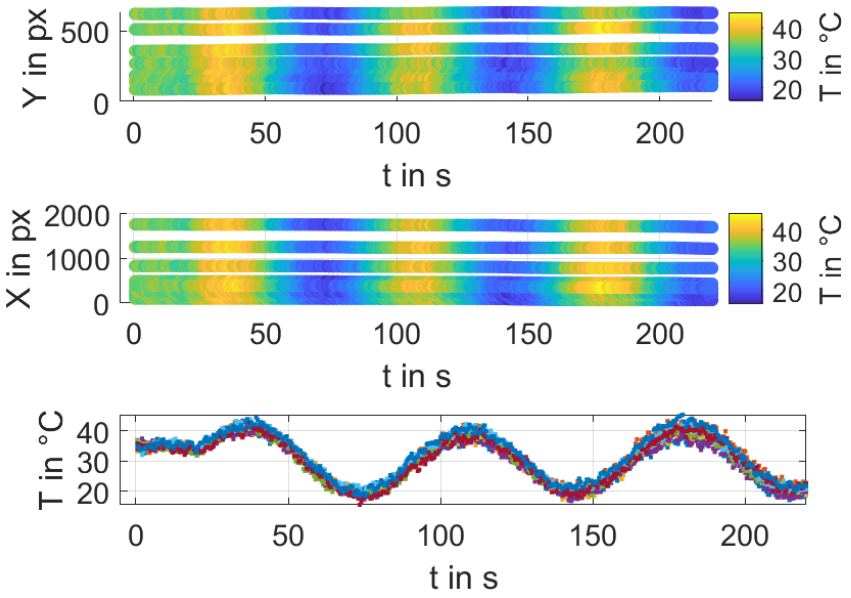

Fig. 5: Reconstruction of the temperature field by the calibration with a sinusoidal set temperature. A second order polynomial for the gradient and offset determined for each particle individually is used.

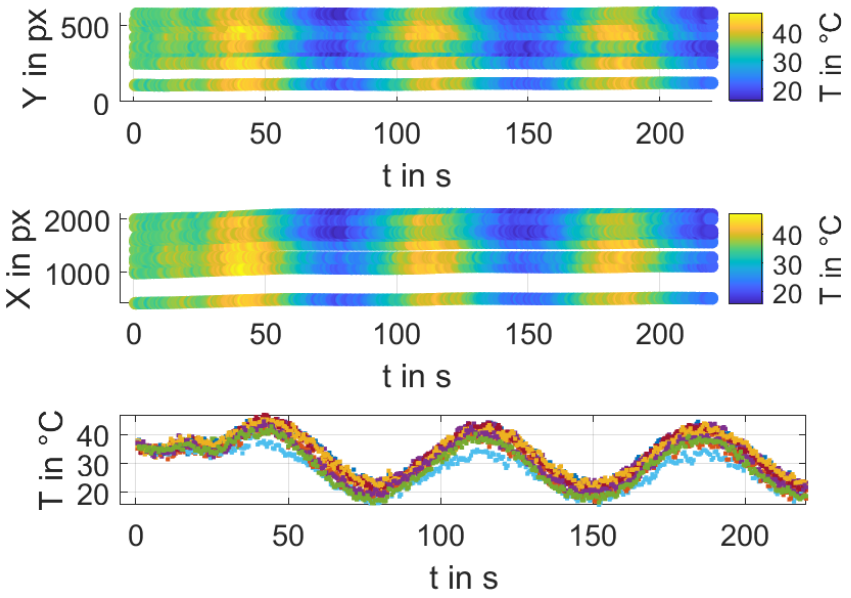

Fig. 6: Application of the calibration derived from one particle distribution to a different set of particles. Reconstruction of the temperature field by the calibration with a sinusoidal set temperature. A second order polynomial for the gradient and offset determined for each particle individually is used.

Preliminary results

The effect of the rolling shutter on the temperature measurements can be immediately seen in Fig. 7. In the upper graph the *y*-position of particles are shown over time. The laser and the sound field were switched on at t = 0 s. An immediate movement of the particles in the y-direction can be seen and within ~ 10 seconds the particles are focused by the acoustic radiation force in the center of the channel. The typical trajectories can also be seen in the middle graph, showing a top view of the system. However, in this case the calibration was performed using the calibration function determined by the above-mentioned calibration procedure from the region where the particle image is located at the beginning of the measurement. By this procedure individual differences for different particles are considered. However, it can be observed that the particles moving from lower *y*-values towards the centre would show an increasing temperature and particles moving from higher *y*-values showing a large temperature

GALA e.V., Karlsruhe, Germany, ISBN 978-3-9816764-9-5

decrease. Both effects are not physical and are caused by the rolling shutter as the time difference between the first and the second frame differs for different *y*-positions. The read out of the camera is from lower *y*-values to higher *y*-values, which means, that the time difference becomes larger for particles moving in positive *y*-direction. Thus, the ratio of I_2/I_1 becomes smaller even if the temperature is constant. This would result in an increase of the measured temperature which is not physical at all and can be seen in the lower graph in Fig. 7.

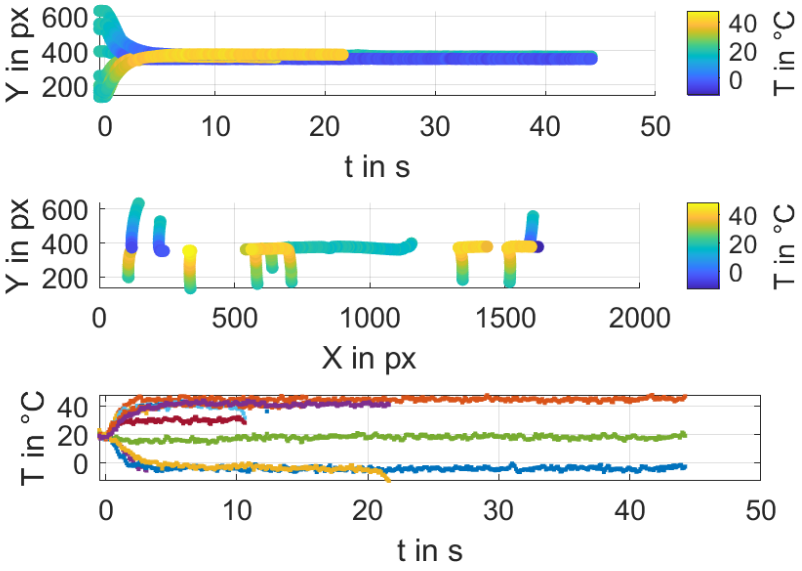

Fig. 7: Particle positions and temperatures taking the calibration parameters from the initial position. It can be seen that the temperature is corrupted by the rolling shutter effect as particles moving in negative y-direction show a temperature decrease and particles moving in positive y-direction a strong increase in temperature.

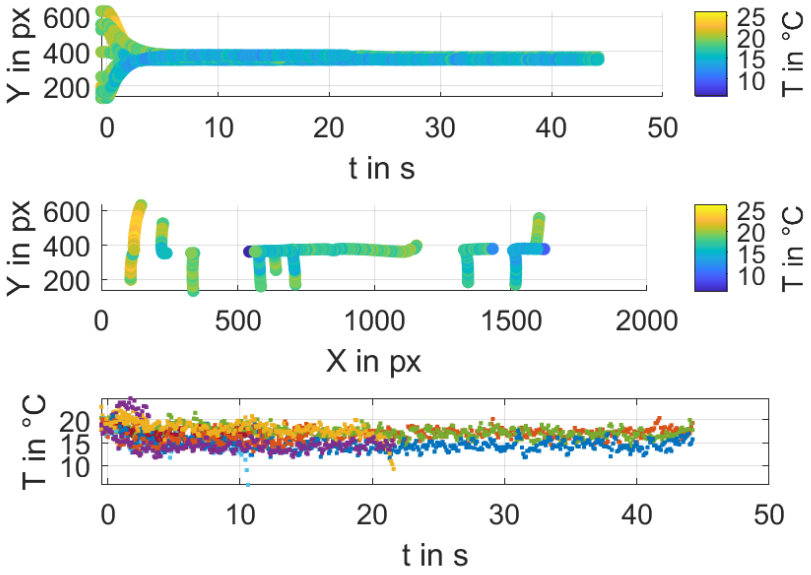

Fig. 8: Particle positions and temperatures taking the calibration parameters in dependence of the position in the field of view. It can be seen that the temperature seems unphysically decreasing when the sound field is switched on and the particles move in y-direction as the calibration parameters change considerably. In general, a slight increase of the temperature for longer time spans can be seen.

For the results shown in Fig. 8, the calibration was taken in dependence of the *x*- and *y*-position. This approach considers the differences due to the rolling shutter and inhomogeneous illumination. However, it does not take into account the individual differences of different particles images. The scatter of

GALA e.V., Karlsruhe, Germany, ISBN 978-3-9816764-9-5

the individual data in the lower graph is therefore high in comparison to the overall temperature level that does not change much during the experiment. Fitting a power law to the mean temperature after the movement of the particles by the acoustic field a slight increase in temperature of ~ 0.3 K within 30 seconds can be determined. This is somehow in correspondence to the additional measurement from the outside by the Pt100 sensor that shows typical temperature increases of 0.2 K for the current experimental procedures.

Conclusion and Outlook

In conclusion, it can be stated that a temperature measurement based on life time imaging was implemented for the thermoacoustic excited flow in a microchannel. Challenges for the technique are the necessity to image through the whole channel, the usage of a rolling shutter camera and individual differences for different particles in the calibration curve. It was shown that a calibration using a sinusoidal set temperature and considering the particle image position allows temperature measurements in a range of 20 to 40°C. However, the uncertainty for individual particles is in the order of ~ 9 K (two times the standard deviation). As the measured temperatures were much lower than expected, further optimization has to be conducted to determine reliable temperature data. These optimizations may include tests with a global shutter camera and repeated calibration measurements to further separate random errors from systematic errors. In addition, experiments using a defocus method to determine the volumetric temperature distribution is planned (Deng et al. 2022).

Acknowledgements

The authors are thankful to Enrico Corrado and Ola Jakobsson for the help in the lab and fruitful discussion. The Swedish Foundation for Strategic Research (Grant No. FFL18-0122) and the European Research Council (ERC) under the European Union's Horizon 2020 research and innovation programmer (Grant Agreement No. 852590) are gratefully acknowledged. CC gratefully acknowledges the financial support by the DFG under grants CI 185/7, CI 185/8 and CI 185/14.

References

R. Barnkob, C. Cierpka, M. Chen, S. Sachs, P. Mäder, M. Rossi (2021) Defocus particle tracking: A comparison of methods based on model functions, cross-correlation, and neural networks, Measurement Science and Technology 32, 094011, DOI: 10.1088/1361-6501/abfef6

Z. Deng, J. König, C. Cierpka (2022) Astigmatism Particle Tracking Velocimetry and Lifetime Imaging using LED and low-speed cameras, Measurement Science and Technology 33, 115301, DOI: 10.1088/1361-6501/ac82da, open access

J. T. Karlsen, P. Augustsson, H. Bruus (2016) Acoustic Force Density Acting on Inhomogeneous Fluids in Acoustic Fields, Phys. Rev. Lett. 117, 114504, DOI: 10.1103/PhysRevLett.117.114504

J. Massing, C.J. Kähler, C. Cierpka (2018) A volumetric temperature and velocity measurement technique for microfluidics based on luminescence lifetime imaging, Experiments in Fluids 59, 163, DOI: 10.1007/s00348-018-2616-y

W. Qiu, J. H. Joergensen, E. Corato, H. Bruus, P. Augustsson (2021) Fast Microscale Acoustic Streaming Driven by a Temperature-Gradient-Induced Nondissipative Acoustic Body Force, Phys. Rev. Lett. 127, 064501, DOI: 10.1103/PhysRevLett.127.064501

S. Sachs, M. Baloochi, C. Cierpka, J. König (2022) On the Influence of acoustic streaming for the particle fractionation in a standing surface acoustic wave field - Part I, Lab on a Chip 22, 2011 - 2027, DOI: 10.1039/d1lc01113h, open access

R. Weser, Z. Deng, V.V. Kondalkar, A.N. Darinski, C. Cierpka, H. Schmidt, J. König (2022) Three-dimensional Heating and Patterning Dynamics of Particles in Microscale Acoustic Tweezers, Lab on a Chip 22, 2886 - 2901, DOI: 10.1039/D2LC00200K

GALA e.V., Karlsruhe, Germany, ISBN 978-3-9816764-9-5